Account for the backscattering anisotropy in lidar returns from dense media

V.V. Veretennikov

Institute of Atmospheric Optics,
Siberian Branch of the Russian Academy of Sciences, Tomsk

Received October 4, 2004

Within the framework of small-angle approximation of the radiative transfer theory, a new equation is derived for the power of lidar return taking into account multiple scattering at small angles and anisotropic single scattering at large angles. It is shown that the solution of the problem can be reduced to calculation of medium irradiance with the preserved complete information about the scattering phase function in the small-angle region and near the backward direction. The technique proposed is used to assess the domain of applicability of the approximation of isotropic backscattering phase function in the problem of airborne sensing of seawaters.

Introduction

By now a considerable progress has been achieved in constructing numerical-analytical models, describing lidar returns with the allowance for multiple scattering. The lidar equation is usually derived taking into account the multiple scattering at small angles and only one event of scattering at large angles.[1–10] However, even in this simplified version, the calculation of the contribution from multiple scattering to the lidar return remains a cumbersome problem in the case that the scattering phase function is variable in the range of angles close to the backward direction.

The problem becomes much simpler if the scattering phase function in the backscattering range is replaced by some average characteristic, which generally depends on both optical characteristics of the medium and geometric parameters of the lidar system.

To describe lidar returns, Bissonnette and Hutt[1,2] proposed a phenomenological model, which considers the multiple scattering as a diffusion process. The backscattering anisotropy in Refs. 1 and 2 is taken into account by introducing a dimensionless coefficients, which characterize the measure of variability of the scattering phase function near the backward direction and can be determined through its averaging by different methods.

Another model of the lidar return[3] is constructed based on a successive consideration of individual events of the scattering at small angles. For every number of scattering events, this model considers "effective" values of the scattering phase function, which are supposed constant and calculated with the aid of the weighted averaging of actual scattering phase functions. A significant part of these models[1–3] is the use of the Gaussian approximation for the small-angle scattering phase function.

More general theory based on the expansion of the radiative transfer equation (RTE) over the multiplicity orders of scattering at large angles and the application of the Green's function method has been developed in Refs. 4 and 5 for the case of isotropic backscatter. Based on the results from Ref. 5, the equations were derived[6,7] for lidar returns that allow for the disperse composition of the medium in sensing the atmosphere and seawaters. These equations are based on the asymptotic properties of signals in the case, when the receiver field of view increases infinitely. This approach allows the small-angle scattering phase function to be replaced in calculations by only one numerical parameter, which is determined by the effective size of particles.

The theory developed in Ref. 5 is generalized and developed in Refs. 8 and 9 with the allowance for anisotropy of the backscattering phase function. However, the practical implementation of the results of Refs. 8 and 9 is significantly complicated due to the need to perform laborious numerical calculations of multiple integrals. In Ref. 10, to facilitate the calculation of the power of backscattered signal by equations from Refs. 8 and 9 when determining the radiation intensity in the medium, it is proposed to use the small-angle diffusion approximation (SDA) of radiative transfer theory. At the same time, it should be taken into account that the information about the fine structure of the light field in the small-angle region is lost upon the transition to SDA, and this is significant for the solution of inverse problems of laser sensing.

Within the framework of the small-angle approximation, this paper proposes a new approach to the approximate consideration of backscattering anisotropy in lidar returns. With the complete information about the scattering phase function in the small-angle region kept, the technique developed

0235-6880/04/12 872-08 $02.00 © 2004 Institute of Atmospheric Optics

reduces the solution of the problem to the calculation of irradiance distribution in the medium, which considerably decreases the computational time.

The technique is applied to assess the effect of the backscattering anisotropy in the calculation of the contribution from multiple scattering in sensing the seawaters. The calculated results make it possible the determination of the applicability limits for the approximation of the isotropic scattering phase function depending on the microphysical properties of the disperse suspended matter in the seawater, the optical thickness of the layer, and the field of view of the lidar receiving system.

1. Formulation of the problem and the scheme of solution

The aim of this section is the mathematical description of the backscattered signal in dense coarse-dispersed media with the allowance for the anisotropy of the scattering phase function near the backward direction. The multiple scattering will be considered within the framework of the small-angle approximation of radiative transfer theory. Since this approach has already gained a sufficient consideration in the literature, including the needed reference material (see, for example, Refs. 11–13), here we will describe only the main stages of the problem solution in the part, which presents new elements.

In solving the problems of radiative transfer through the media with anisotropic scattering in the coefficient of directed light scattering $\beta(\gamma) = \sigma x(\gamma)$, where σ is the scattering coefficient, and $x(\gamma)$ is the scattering phase function normalized as $\int_{4\pi} x(\gamma)\,d\Omega = 1$, it is a usual practice to separate the forward peak of $\beta_1(\gamma) = \sigma_1 x_1(\gamma)$, which describes the scattering at small angles. Designating the residual part as $\beta_2(\gamma) = \beta(\gamma) - \beta_1(\gamma)$, we can write the following equation for the scattering phase function:

$$x(\gamma) = a_1 x_1(\gamma) + a_2 x_2(\gamma) \qquad (1)$$

with the weighting coefficients $a_1 = \sigma_1/\sigma$ and $a_2 = \sigma_2/\sigma$, $\sigma = \sigma_1 + \sigma_2$. As was already mentioned in the Introduction, theory of laser sensing usually takes into account multiple scattering at small angles and only one event of the scattering at large angles. This leads to the solution of the radiative transfer equation with the source density function Q in the form

$$Q(\mathbf{R}, \mathbf{n}) = \sigma_2 \int_{4\pi} x_2(\mathbf{n}, \mathbf{n}') I_1(\mathbf{R}, \mathbf{n}')\,d\mathbf{n}', \qquad (2)$$

where $\mathbf{R} = (x,y,z)$ is the radius vector of a point; $\mathbf{n}$ is the unit direction vector; the function $I_1(\mathbf{R},\mathbf{n}')$ describes the spatial-angular intensity distribution of the radiation at the forward propagation of the sounding pulse within the framework of the small-angle approximation. In practice, the scattering phase function in Eq. (2) is often substituted by some effective characteristic, assuming, for example, $x_2(\gamma) \approx x_2(\pi)$. This substitution does not lead to large distortions in the case of smooth behavior of $x_2(\gamma)$ near the backward direction and at small receiver's field of view.

Within the framework of the small-angle approximation, the intensity $I_1(\mathbf{R}, \mathbf{n}')$ has a significant value only in a small vicinity of the initial direction of the light beam propagation, in the medium. Let this direction coincide with the direction of the axis Oz. Then in the case that the angle $\gamma = (\mathbf{n}\hat{}\mathbf{n}')$ between the directions $\mathbf{n}$ and $\mathbf{n}'$ is close to π and, consequently, the angle $\theta = \pi - \gamma$ is small, we can write the approximate equation

$$\theta \cong |\mathbf{n}_\perp + \mathbf{n}'_\perp|, \qquad (3)$$

where $\mathbf{n}_\perp$ and $\mathbf{n}'_\perp$ are the projections of the vectors $\mathbf{n}$ and $\mathbf{n}'$ onto the plane, orthogonal to the axis Oz. On these assumptions, the right-hand side of Eq. (2) can be presented as a double integral

$$Q(\mathbf{R},\mathbf{n}_\perp) = \sigma_2 \iint x_\pi(|\mathbf{n}_\perp + \mathbf{n}'_\perp|) I_1(\mathbf{R},\mathbf{n}'_\perp)\,d\mathbf{n}'_\perp, \qquad (4)$$

where $x_\pi(\theta) = x_2(\pi - \theta)$. The following procedure of derivation of the solution is based on the ordinary application of the method of Green's function and the optical reciprocity theorem. To facilitate the reasoning, we will consider below the problem for the case that the medium is irradiated with a point source of a pulsed unidirectional (PUD) radiation, which generates the following intensity distribution on the medium boundary $z = 0$

$$I(\mathbf{r}_\perp, z = 0, \mathbf{n}_\perp, t) = \delta(\mathbf{n}_\perp - \mathbf{n}_{0\perp})\delta(\mathbf{r}_\perp - \mathbf{r}_{0\perp})\delta(t) \qquad (5)$$

at $\mathbf{n}_{0\perp} = 0$, $\mathbf{r}_{0\perp} = 0$. The extension to the case of an arbitrary intensity distribution on the boundary $I(\mathbf{r}_\perp, z = 0, \mathbf{n}_\perp, t)$ presents no problems. Thus, the function

$$I_1(\mathbf{r}_\perp, z, \mathbf{n}'_\perp, t) =$$

$$= G(\mathbf{r}_{0\perp}, z = 0, \mathbf{n}_{0\perp} \to \mathbf{r}_\perp, z, \mathbf{n}'_\perp)\delta(t - z/c) \qquad (6)$$

in Eq. (4) is simply the Green's function for RTE in the small-angle approximation with the boundary condition (5). The small-angle Green's function of the stationary problem $G(\mathbf{r}_{0\perp}, z = 0, \mathbf{n}_{0\perp} \to \mathbf{r}_\perp, z, \mathbf{n}'_\perp)$ has a sharp peak in the direction $\mathbf{n}'_\perp = \mathbf{n}_{0\perp}$ of the light beam irradiating the medium and decreases fast as the angle $\gamma' = |\mathbf{n}'_\perp|$ deviates from zero. The scattering phase function $x_\pi(|\mathbf{n}_\perp + \mathbf{n}'_\perp|)$, to the contrary, changes much more slowly. Therefore, we can expect that substitution of the small-angle Green's function by the two-dimensional δ-function

$$G(\mathbf{r}_{0\perp}, z = 0, \mathbf{n}_{0\perp} \to \mathbf{r}_\perp, z, \mathbf{n}'_\perp) = E_1(\mathbf{r}_\perp)\delta(\mathbf{n}'_\perp - \mathbf{n}_{0\perp}) \qquad (7)$$

with the normalizing factor

$$E_1(\mathbf{r}_\perp) = \iint G(\mathbf{r}_{0\perp}, z = 0, \mathbf{n}_{0\perp} \to \mathbf{r}_\perp, z, \mathbf{n}'_\perp)\mathrm{d}\mathbf{n}'_\perp \quad (8)$$

does not lead to a large error in the integral (4). It can be seen from Eq. (8) that the normalizing factor $E_1(\mathbf{r}_\perp)$ is the spatial irradiance, generated by the PUD radiation (5) at the point $\mathbf{r}_\perp$. Taking into account the approximation (7), we obtain the following equation for the source function of the stationary problem:

$$Q(\mathbf{R}, \mathbf{n}_\perp) = \sigma_2 x_\pi(|\mathbf{n}_\perp|) E_1(\mathbf{r}_\perp). \quad (9)$$

Assume then that the observations in lidar measurements are conducted in the plane $z = 0$. Then, using the Green's function method and the optical reciprocity theorem, we can write the following equation for the light field in the observation plane, corresponding to the source density $Q(\mathbf{R}, \mathbf{n}_\perp)$ [Eq. (9)]:

$$I(\mathbf{r}_\perp, z = 0, \mathbf{n}_\perp, t) = (\sigma_2 c/2) \iint_S E_1(\mathbf{r}'_\perp)\mathrm{d}\mathbf{r}'_\perp \times$$

$$\times \iint x_\pi(|\mathbf{n}'_\perp|) G(\mathbf{r}_\perp, z = 0, -\mathbf{n}_\perp \to \mathbf{r}'_\perp, z', -\mathbf{n}'_\perp)\mathrm{d}\mathbf{n}'_\perp. \quad (10)$$

Here S is the integration plane $z' = ct/2$. By analogy with the case considered above, in the integration over the angular variable in Eq. (10), the Green's function is approximated as:

$$G(\mathbf{r}_\perp, z = 0, -\mathbf{n}_\perp \to \mathbf{r}'_\perp, z', -\mathbf{n}'_\perp) = E_2 \delta(\mathbf{n}'_\perp - \mathbf{n}_\perp), \quad (11)$$

where

$$E_2(\mathbf{r}_\perp, -\mathbf{n}_\perp \to \mathbf{r}'_\perp, z') =$$

$$= \iint G(\mathbf{r}_\perp, z = 0, -\mathbf{n}_\perp \to \mathbf{r}'_\perp, z', -\mathbf{n}'_\perp)\mathrm{d}\mathbf{n}'_\perp \quad (12)$$

is the spatial irradiance generated at the point $\mathbf{R} = (\mathbf{r}'_\perp, z')$ by a fictitious PUD radiation from a source located at the point $\mathbf{r}_\perp$ of the plane $z = 0$ and emitting along the direction $-\mathbf{n}_\perp$. This leads to the following equation for the light field intensity distribution in the plane $z = 0$:

$$I(\mathbf{r}_\perp, z = 0, \mathbf{n}_\perp, t) = (\sigma_2 c/2) x_\pi(|\mathbf{n}_\perp|) \times$$

$$\times \iint_S E_1(\mathbf{r}'_\perp) E_2(\mathbf{r}_\perp, -\mathbf{n}_\perp \to \mathbf{r}'_\perp, z')\mathrm{d}\mathbf{r}'_\perp. \quad (13)$$

In the small-angle approximation, the property of invariance is true for the spatial irradiance:

$$E_2(\mathbf{r}_\perp, \mathbf{n}_\perp \to \mathbf{r}'_\perp, z') = E_0(|\mathbf{r}'_\perp - \mathbf{r}_\perp - z'\mathbf{n}_\perp|), \quad (14)$$

where $E_0(\mathbf{r}_\perp)$ is the scattering function of the light beam (SFB), that is, the irradiance distribution in the plane z, generated by the PUD radiation from a source located at the origin of coordinates and emitting along the direction of the axis Oz. Taking into account the property (14), the integral in Eq. (13) takes the form of the two-dimensional convolution in the plane S:

$$I(\mathbf{r}_\perp, z = 0, \mathbf{n}_\perp, t) = (\sigma_2 c/2) x_\pi(|\mathbf{n}_\perp|) \times$$

$$\times \iint_S E_1(\mathbf{r}'_\perp) E_0(|\mathbf{r}_\perp - z'\mathbf{n}_\perp - \mathbf{r}'_\perp|)\mathrm{d}\mathbf{r}'_\perp. \quad (15)$$

The application of the convolution theorem to Eq. (15) finally yields

$$I(\mathbf{r}_\perp, z = 0, \mathbf{n}_\perp, t) = (c/4\pi)\sigma_2 x_\pi(|\mathbf{n}_\perp|) \times$$

$$\times \int_0^\infty \nu J_0(\nu|\mathbf{r}_\perp - z'\mathbf{n}_\perp|) F(\nu)\mathrm{d}\nu, \quad (16)$$

where

$$F(\nu) = \exp\left[-2\tau(z) + g(\nu)\right] \quad (17)$$

is the optical transfer function (OTF) of the fictitious medium, whose extinction and scattering coefficients are twice as high as their true values;

$$\tau(z) = \int_0^z \varepsilon(s)\,\mathrm{d}s; \quad g(\nu) = 2\int_0^z \sigma_1(z - s)\tilde{x}_1(\nu s)\mathrm{d}s. \quad (18)$$

Equations (16)–(18) employ the following designations: ν is the spatial frequency; $J_0(.)$ is the first-kind zero-order Bessel function; $\tau(z)$ and $\varepsilon(z)$ are the optical thickness and the extinction coefficient; $\tilde{x}_1(p)$ is the Hankel transform of the small-angle scattering phase function.

Accurate to a constant factor before the integral sign, the structure of Eq. (16) resembles the equation for the intensity of light field generated by an isotropic radiation from a point source.[13] The main difference from the case mentioned above is the explicit dependence of the backscattering phase function $x_\pi(|\mathbf{n}_\perp|)$ on the angular coordinate. Using Eq. (16), we can easily calculate the power of the lidar return for the given parameters of the receiving system. The following analysis will be restricted to the case that the sensitivity function of the lidar receiving system has a circular symmetry and the stepwise behavior over the variables $r = |\mathbf{r}_\perp|$ and $\gamma = |\mathbf{n}_\perp|$:

$$D(r, \gamma) = U(R_\mathrm{r} - r)U(\gamma_\mathrm{r} - \gamma), \quad (19)$$

where $U(.)$ is the unit stepwise function; R_r and γ_r are the radius of the entrance pupil and the halved field of view of the receiving system. Under these conditions, if the lidar emits a δ-pulse with the unit energy, the lidar return power detected at the time $t = 2z/c$ is described by the following equation:

$$P(z) = (c\pi)\sigma_2(z) \int_0^{\gamma_\mathrm{r}} x_\pi(\gamma) B(z\gamma)\gamma\mathrm{d}\gamma, \quad (20)$$

where

$$B(r) = \frac{1}{2\pi}\int_0^\infty \nu J_0(r\nu) F(\nu)\tilde{U}(\nu, R_\mathrm{r})\mathrm{d}\nu; \quad (21)$$

$$\tilde{U}(\nu, R_r) = S_r \frac{2J_1(\nu R_r)}{\nu R_r}$$

is the Hankel transform of the first co-factor in Eq. (19); $S_r = \pi R_r^2$ is the area of the entrance pupil of the receiving system. At a sufficiently small size of the entrance pupil $\tilde{U}(\nu, R_r) \to S_r$, and the function $B(r) = S_r E(r)$ coincides, accurate to the constant factor S_r, with the SFB $E(r)$ in the fictitious medium.

Separation of signals due to single and multiple scattering

For the following analysis of the lidar return $P(z)$, it is convenient, as usually, to separate the components due to single and multiple scattering in Eq. (20). These components correspond to the following terms in the OTF

$$F(\nu) = F_0 + F_{sc}(\nu),$$

where $F_0 = e^{-2\tau(z)}$. After the appropriate substitution in Eq. (21), we obtain the following equation for the lidar return in the single scattering approximation with the allowance for the angular dependence of the single scattering function near the backward direction:

$$P_1(z) = (c\pi) e^{-2\tau(z)} \int_0^{R_r/z} \beta_\pi(z, \gamma) \gamma d\gamma, \qquad (22)$$

where

$$\beta_\pi(z, \gamma) = \sigma_2(z) x_\pi(\gamma) \qquad (23)$$

is the coefficient of directed scattering, $\beta_\pi(\gamma) = \beta(\pi - \gamma)$. Equation (22) is derived under condition that $z\gamma_r > R_r$, determining the far sensing zone,[3] which is of greatest practical interest.

In the case that the backscattering phase function remains constant within the domain of integration in Eq. (22), that is, $\beta_\pi(z, \gamma) = \beta_\pi(z)$, Eq. (22) takes the standard form:

$$P_1(z) = (c/2) S_r z^{-2} \beta_\pi(z) e^{-2\tau(z)}. \qquad (24)$$

For the most real situations (except for, for example, the mirror reflection from crystal particles), the last assumption is valid, which justifies the applicability of the lidar equation in the form (24) within the framework of the single scattering approximation.

The equation for the contribution of multiple scattering, related to $P_1(z)$, to the lidar return:

$$m = [P(z) - P_1(z)] / P_1(z), \qquad (25)$$

can be easily obtained from general equations (20) and (21) with $F_{sc}(\nu)$ substituted for $F(\nu)$. With the allowance made for expression (24), this leads to the following equation:

$$m(\gamma_r) = \frac{2\pi}{F_0} \int_0^{z\gamma_r} \hat{x}(\rho/z) E_{sc}(\rho) \rho d\rho, \qquad (26)$$

where the function

$$\hat{x}(\gamma) = x_\pi(\gamma) / x_\pi(0) \qquad (27)$$

describes the angular variability of $x_\pi(\gamma)$ with respect to the backward direction, and the function $E_{sc}(\rho)$ is the SFB component, corresponding to the scattered component $F_{sc}(\nu)$ at the direct propagation of light through a fictitious medium. At $x_\pi(\gamma) = \text{const}$, $0 \le \gamma \le \gamma_r$, the function $m(\gamma_r)$ (26) becomes independent of the scattering phase function $x_\pi(\gamma)$ and Eq. (26) completely coincides with the solution obtained earlier for the case of the isotropic backscattering phase function.[13] In combination with the Eq. (24), Eq. (26) gives full description of the lidar return formed due to multiple scattering at small angles and the single anisotropic scattering, taken into account near the backward direction.

2. Results of numerical simulation

In this Section, we will consider some examples of the function $m(\gamma_r)$ (26) calculated taking into account the backscattering anisotropy and will compare them with similar results obtained assuming $x_\pi(\gamma) = \text{const}$ in application to airborne lidar sensing of seawaters.

The earlier results[14] of investigation of the scattering phase functions for radiation at the wavelength $\lambda = 0.532$ μm by particles of suspended matter in seawaters, formed by two fractions: of mineral (t-fraction) and organic (b-fraction) origin served the prerequisites for the detailed consideration of this case.

Let us remind briefly the conditions of the numerical simulation considered in Ref. 14. The disperse composition of the t-fraction was characterized by the power-law particle size distribution:

$$s_t(r) = \begin{cases} A_{t0}, & 0.01 \le r \le 0.05 \ \text{μm}, \\ A_t r^{-\nu}, & 0.05 \le r \le 2 \ \text{μm} \end{cases} \qquad (28)$$

with the exponent $\nu = 1$–4. The relative refractive index of the t-fraction particles was $n_t = 1.15$. The size-distribution function for the b-fraction particles was simulated using a modified gamma-distribution

$$s_b(r) = A_b \left(\frac{r}{r_m}\right)^\alpha \exp\left\{-\frac{\alpha}{\gamma}\left[\left(\frac{r}{r_m}\right)^\gamma - 1\right]\right\} \qquad (29)$$

with the variable modal radius $r_m = 5$–15 μm and the fixed parameters $\alpha = 8$ and $\gamma = 3$. The values of the relative refractive index n_b were set within the range from 1.03 to 1.05. The weighting factors A_t and A_b in the distributions $s_t(r)$ and $s_b(r)$ were chosen in such a way that they ensured the given ratio between the contributions of these fractions to the total scattering coefficient $\sigma = \sigma_t + \sigma_b$.

The total scattering phase function for both of the fractions was determined by the equation

$$x(\theta) = px_t(\theta) + (1 - p)x_b(\theta), \qquad (30)$$

where $x_t(\theta)$ and $x_b(\theta)$ are the scattering phase functions of the t- and b-fractions of the suspended matter, respectively; the parameter $p = \sigma_t/\sigma$ determines the relative contribution of the t-fraction to the total scattering coefficient σ. Typical example of the angular dependence $x(\theta)$, calculated by Eq. (30) for the microstructure model of the suspended matter described by Eqs. (28) and (29), is shown in Fig. 1.

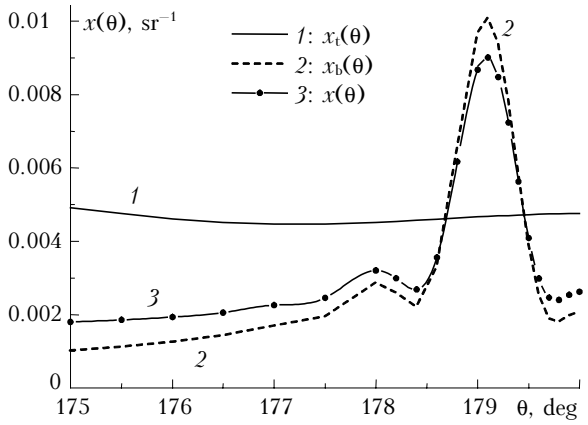

Fig. 1. Examples of calculated scattering phase functions $x_t(\theta)$ at $\nu = 2$ (curve *1*), $x_b(\theta)$ for the modal radius $r_m = 10$ μm (curve *2*) and their weighted sum $x(\theta)$ at $p = 0.2$ (curve *3*).

The numerical calculations made have allowed us to find the following properties of the scattering phase functions of the suspended matter.[14] First, the isotropic behavior in the angular range from 175 to 180° is mostly inherent in the scattering phase function of fine particles belonging to the t-fraction. Second, the angular dependences of the scattering phase functions for coarse particles of the b-fraction have a diffraction peak (glory) at $\theta > 179°$ (seen in Fig. 1), whose position and amplitude depend on the particle size and the refractive index. Consequently, we can expect that under certain conditions the observed anisotropy of the scattering phase function near 180° will manifest itself in the behavior of the lidar return with multiple scattering taken into account.

In the numerical simulation, whose results are presented below, the scheme and conditions of sensing were taken analogous to those described in Ref. 15. It was assumed that the sensing of the water depth is carried out by a lidar located at the height $H = 300$ m above the sea level; the signal was detected from the depth of 20 m; the receiver's field of view γ_r varied from 0 to 15 mrad.

To take into account the "atmosphere–sea" interface, the parameter z in Eq. (26) was replaced, as in Ref. 15, by $l = H + (z - H)/n_w$, where n_w is the refractive index of the seawater. In addition, the argument γ of the scattering phase function in Eq. (26) should be replaced by γ/n_w.

The ratio $m(\gamma_r)$ calculated as a function of the detector field of view γ_r for these conditions is shown in Figs. 2–5. Figure 2 depicts the behavior of the function $m(\gamma_r)$ at different optical thickness of the layer $\tau = 1$–4 for the scattering phase function $x(\theta)$ shown in Fig. 1. The combination of the microstructure parameters ($\nu = 2$, $r_m = 10$ μm, $p = 0.2$), for which the dependences $m(\gamma_r)$ shown in Fig. 2 were obtained, corresponds to the situation that the b-fraction of the suspended particles plays the leading role in the scattering phase function both in the backward direction[14] and in the small-angle region.[16]

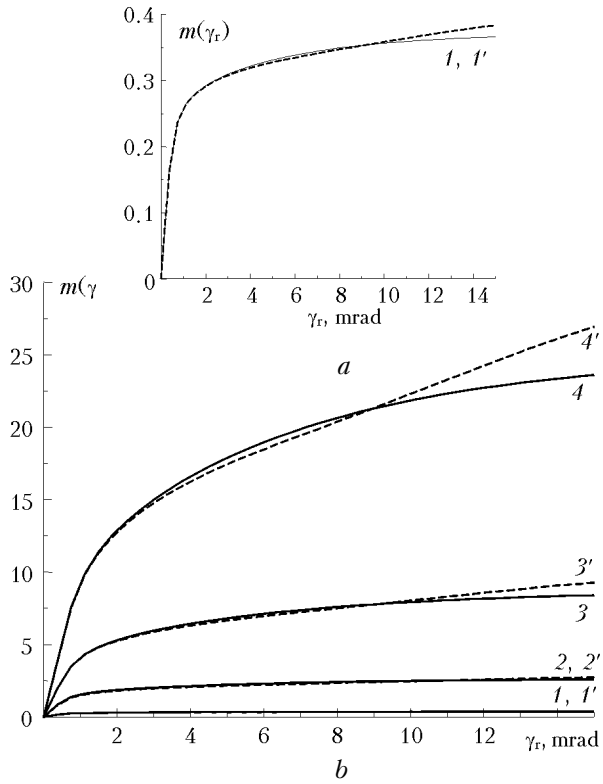

Fig. 2. Effect of the optical thickness on the ratio $m(\gamma_r)$ neglecting (curves *1*–*4*) and taking into account (curves *1′*–*4′*) the backscattering anisotropy: $\tau = 1$ (*1*, *1′*), 2 (*2*, *2′*), 3 (*3*, *3′*), and 4 (*4*, *4′*).

As can be seen from Fig. 2, the anisotropy in the backward direction, caused by the diffraction peak in the scattering phase function $x_b(\theta)$ at the angle $\theta_1 = 179.1°$, manifests itself in $m(\gamma_r)$ at sufficiently large γ_r.

The maximum discrepancy between the curves $m(\gamma_r)$ calculated with and without the regard for the backscattering anisotropy is observed at the largest values of the considered field of views ($\gamma_r = 15$ mrad). It amounts to 4.4% at the low optical density of the layer ($\tau = 1$) and achieves about 12% as τ increases up to 4. This increase in the role of the backscattering anisotropy with the increasing optical

thickness has a simple physical explanation, connected with the broadening of SFB $E_{sc}(\rho)$, which serves a weighting function of the scattering phase function $x_\pi(\gamma)$ in Eq. (26), due to multiple scattering.

The effect of the backscattering anisotropy can be neglected for the angles $\gamma_r < 10.5$ mrad. The error in this case does not exceed 3% at $\tau < 4$.

Figure 3 illustrates the effect of the disperse composition of the b-fraction of the suspended matter on the behavior of $m(\gamma_r)$ with the backscattering anisotropy taken into account. In this case, two opposite tendencies should be taken into account. As was shown in Ref. 14, the contribution coming from the b-fraction particles to the backscatter increases with the increase of their size. As this takes place, the amplitude of the diffraction peak near the backward direction grows, and the position of the peak shifts toward the scattering angle $\theta = 180°$. These factors obviously enhance the effect of the backscattering anisotropy on the angular dependence of $m(\gamma_r)$ with the increase of the modal radius r_m of the b-fraction particles.

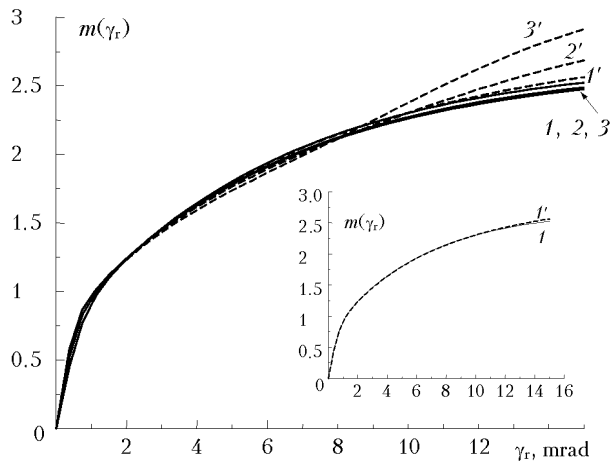

Fig. 3. The ratio $m(\gamma_r)$, calculated with (curves *1′–3′*) and without (curves *1–3*) the regard for the backscattering anisotropy, at the modal radius of the b-fraction particles $r_m = 8$ (*1*, *1′*), 10 (*2*, *2′*), and 12 μm (*3*, *3′*).

At the same time, it should be kept in mind that the growth of the particles leads to narrowing of SFB $E_{sc}(\rho)$ due to the increasing forward peak of the small-angle scattering phase function. As a result, the anisotropic part of $x_\pi(\gamma)$ will be present in the dependence $m(\gamma_r)$ (26) with the smaller weight. The resultant effect of these factors on the variability of $m(\gamma_r)$ can be estimated only numerically (a typical case is shown in Fig. 3).

It can be seen from Fig. 3 that if the modal particle radius r_m does not exceed 8 μm, the effect of the backscattering anisotropy on the behavior of the function $m(\gamma_r)$ is negligibly small all over the considered range of the field of view γ_r. The approximation of the isotropic backscatter is acceptable, within the error smaller than 2.5% for $\gamma_r < 9$ mrad for particles with the modal radius $r_m \le 12$ μm. For large γ_r, the neglect of backscattering anisotropy leads to the increase of the error in the calculation of $m(\gamma_r)$, achieving, for example, 15% at $\gamma_r = 15$ mrad and $r_m = 12$ μm.

Figure 4 illustrates the effect of the microstructure parameters of the t-fraction particles on the behavior of $m(\gamma_r)$. As was shown in Ref. 14, the scattering phase function of the t-fraction particles near the backward direction is quasi-isotropic, and the increase of the parameter ν in the distribution (28) leads to the increasing role of this fraction in the backscatter. As a result (Fig. 4), at large values of ν the backscattering anisotropy only little manifests itself in the behavior of the function $m(\gamma_r)$. From analysis of the data presented in Fig. 4 it follows that in the case under consideration, as before, the effect of the backscattering anisotropy for the fields of view $\gamma_r < 11$ mrad can be neglected. The error in this case is no higher than 3%.

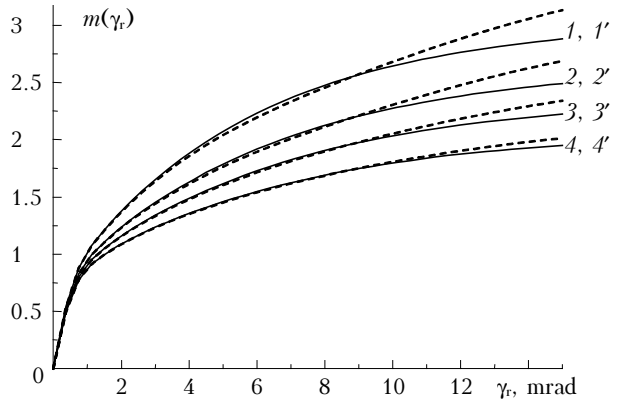

Fig. 4. Ratio $m(\gamma_r)$, neglecting (solid curves) and taking into account (dashed curves) the backscattering anisotropy with the parameter ν of the size distribution of the t-fraction particles: ν = 1 (*1*, *1′*), 2 (*2*, *2′*), 2.5 (*3*, *3′*), and 3 (*4*, *4′*).

Finally, Fig. 5 shows the parametric family of the functions $m(\gamma_r)$, obtained at different contribution p [Eq. (30)] of the t-fraction particles to the light scattering. From the viewpoint of the effect of the backscattering anisotropy on the dependences $m(\gamma_r)$, this example is interesting, because it clearly demonstrates the opposite tendencies, connected with the role of the b-fraction in the forward and backward scattering.

Indeed, at $p = 0$, that is, when the mixture is formed by large particles of organic origin, the scattering phase function has the most pronounced anisotropy both in the small-angle region[16] and at scattering at angles near $\theta = 180°$ (see Fig. 1, curve *2*). However, because of the strong forward peak of the small-angle part of the scattering phase function, the width of the function $E_{sc}(\rho)$ appears insufficient for the diffraction peak of the scattering phase function $x_\pi(\gamma)$, observed in Fig. 1, to affect the formation of the function $m(\gamma_r)$ (26). As a result, the

discrepancy between the curves *1* and *1′* in Fig. 5, obtained, respectively, without and with the regard for the angular dependence $x_\pi(\gamma)$ at $p = 0$, proves to be insignificant (less than 1.6%).

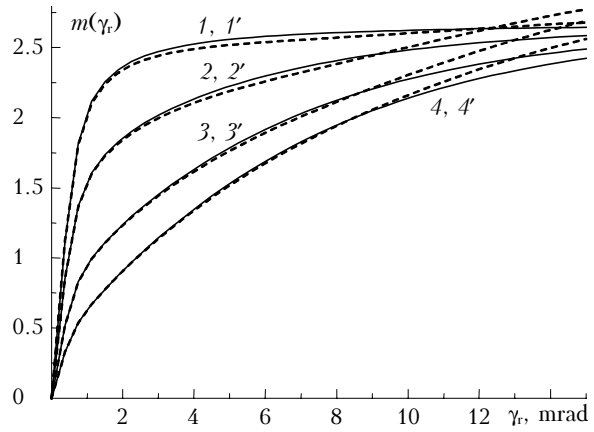

Fig. 5. The ratio $m(\gamma_r)$, calculated with (dashed curves) and without (solid curves) the regard for the backscattering anisotropy at different relative contributions p of the mineral fraction to the total light extinction: $p = 0$ (*1*, *1′*), 0.2 (*2*, *2′*), 0.5 (*3*, *3′*), and 0.7 (*4*, *4′*).

The appearance of the fine t-fraction in the suspended matter leads to broadening of the small-angle peak of the scattering phase function and SFB $E_{sc}(\rho)$ and, as a consequence, to a larger contribution of the diffraction peak of the scattering phase function $x_\pi(\gamma)$ at the periphery of the angular dependence $m(\gamma_r)$. As can be seen from the comparison of the curves *2* and *2′* in Fig. 5, this factor begins to play a marked role already at small values of the parameter p. However, further increase of the parameter p from 0.2 to 0.7 does not affect significantly the role of the backscattering anisotropy in the behavior of the function $m(\gamma_r)$. This is connected with the fact that as the parameter p increases, the scattering phase function $x_\pi(\gamma)$ becomes increasingly smoother[14] and compensates for this effect in the behavior $m(\gamma_r)$. The maximum difference between the dependences $m(\gamma_r)$, calculated with and without the regard for the angular dependence $x_\pi(\gamma)$, amounts to 5–7% at $0.2 \le p \le 0.7$. Thus, in the most cases the relation between the b- and t-fractions proves to be an insignificant factor when taking into account the backscattering anisotropy in the behavior of the function $m(\gamma_r)$.

Conclusions

Within the framework of the small-angle approximation of the radiative-transfer theory, a new equation is obtained for the lidar return power taking into account the multiple scattering at small angles and the single anisotropic scattering at large scattering angles. The account for the single scattering at large angles was based on the solution of RTE with the source density function in the form of the integral of the small-angle Green's function multiplied by the large-angle scattering phase function over the solid angle. The RTE solution has been obtained with the use of the Green's function method and the optical reciprocity theorem.

The principal assumption used in the derivation of the new lidar equation consisted in the δ-approximation of the Green's function in terms of the angular coordinate. Due to this assumption, we significantly simplified the solution, which reduces in this case to the calculation of the irradiance distribution in the medium.

The assumption of the backscattering isotropy considerably simplifies the solution of the inverse problems of laser sensing of dense media taking into account multiple scattering. The theory developed allows the validity of this assumption to be checked for schemes and conditions of lidar experiments.

To test this approach, in this paper the approximation of the isotropic backscattering phase function is applied to the description of the lidar return signal during the airborne sensing of seawaters. For this purpose, the scattering properties were simulated by calculating the scattering phase functions in the case of light scattering by seawaters containing suspended particles of two fractions: of mineral and organic origin. The anisotropy of the scattering phase function showed itself in the diffraction peak, whose amplitude and position in the angular range $\theta > 179°$ depended on the microstructure parameters of the suspended matter.

The analysis of the results of the calculations performed showed that

1. In describing lidar return signals with the field of view ranging within $\gamma_r < 9$–11.5 mrad, it is possible to use the approximation of the isotropic backscattering phase function; the error in this case does not exceed 2.5–3% with the microstructure parameters of the disperse suspended matter varying widely and the optical thickness $\tau < 4$.

2. The larger the modal radius of the b-fraction particles and the higher the optical thickness of the medium, the more significant is the increase in the effect of the backscattering anisotropy with the increasing receiver's field of view.

3. The role of the backscattering anisotropy in the formation of the lidar return signals weakly depends on the relation between the contributions of the two fractions to the total scattering coefficient.

References

1. L.R. Bissonnette, Appl. Opt. **35**, No. 33, 6449–6465 (1996).
2. L.R. Bissonnette and D.L. Hutt, Appl. Opt. **34**, No. 30, 6959–6975 (1995).
3. E.W. Eloranta, Appl. Opt. **37**, No. 12, 2464–2472 (1998).
4. B.V. Ermakov and Yu.A. Il'inskii, Izv. Vyssh. Uchebn. Zaved. SSSR, Radiofiz. **12**, No. 5, 694–701 (1969).

5. L.S. Dolin and V.A. Savel'ev, Izv. Akad. Nauk SSSR, Fiz. Atmos. Okeana **7**, No. 5, 505–510 (1971).
6. V.V. Veretennikov, in: *Abstracts of Reports Presented at III Interrepublic Symp. on Atmospheric and Ocean Optics*, Tomsk (1996), pp. 25–26.
7. V.V. Veretennikov, Proc. SPIE **3983**, 260–270 (1999).
8. I.L. Katsev, E.P. Zege, A.S. Prikhach, and I.N. Polonskii, in: *Abstracts of Reports Presented at II Interrepublic Symp. on Atmospheric and Ocean Optics*, Tomsk (1995), Part 1, pp. 105–106.
9. E.P. Zege, I.L. Katsev, and I.N. Polonskii, Izv. Ros. Akad. Nauk, Fiz. Atmos. Okeana **34**, No. 1, 45–50 (1998).
10. V.V. Barun, Izv. Ros. Akad. Nauk, Fiz. Atmos. Okeana **33**, No. 4, 500–506 (1997).
11. A.S. Monin, ed., *Ocean Optics*. Vol. 1. *Physical Ocean Optics* (Nauka, Moscow, 1983), 372 pp.
12. E.P. Zege, A.P. Ivanov, and I.L. Katsev, *Image Transfer in a Scattering Medium* (Nauka i Tekhnika, Minsk, 1985), 327 pp.
13. V.E. Zuev, V.V. Belov, and V.V. Veretennikov, *Systems Theory in Optics of Disperse Media* (Spektr, Tomsk, 1997), 402 pp.
14. V.V. Veretennikov, Atmos. Oceanic Opt. **17**, No. 9, 681–685 (2004).
15. V.V. Veretennikov, Atmos. Oceanic Opt. **15**, No. 12, 1120–1125 (2002).
16. V.V. Veretennikov, Atmos. Oceanic Opt. **14**, No. 2, 146–152 (2001).